Minimization of Current Stress on the Grid Synchronization of Doubly-fed Induction Generators for Wind Power Generation

K.C. Wong   S.L. Ho   K.W.E. Cheng

Department of Electrical Engineering, The Hong Kong Polytechnic University, Hong Kong
E-mail: k.c.wong@polyu.edu.hk

Abstract - Doubly-fed induction generator (DFIG) is the most common type of generators for wind power generation, because of their high energy yield and the possibility of generating power at variable speeds. For most papers in literature, only the synchronization and power generation of DFIGs, but not the transition between them, are discussed. This paper presents a method to control the transition of DFIGs from synchronization to power generation, in order to minimize the peak current during the transition so as to reduce the impact of synchronization on the power system. In this paper the mathematical model of DFIGs for synchronization, transition, and power generation are firstly described. Then the effects of the time difference between the state transition of the controllers and the closing of the stator side contactors and associated current stresses are investigated. A real-time detection method to determine the optimal time for controller state transition is proposed. Simulation and experimental validations confirm that the current stress is greatly reduced if the time difference is minimized using the proposed method.

Keywords - Induction generator, synchronization, variable speed generation

I. Introduction

Variable speed wind power generation is popular in the industry because variable speed operation of the generators could maximize the energy being captured [1]. Among the various types of variable speed generator, doubly-fed induction generator (DFIG) is the most common [2] because of their large operating speed range, low power rating of the power electronic converters[3], and the feasibility of controlling the real and reactive power independently.

Most co-researchers working on DFIGs focus on the closed-loop power control of DFIGs [4] including field-oriented control (FOC)[5],[6] direct torque control (DTC)[7], [8] and direct power control (DPC) [9], [10]. In FOC, cascaded control loops compose of inner current control loops as well as outer torque and reactive power control loops [5] or outer real and reactive power control loops [6]. In DTC and DPC, reactive power, and torque or real power are computed and controlled directly, with hysteresis variable switching frequency controllers [7], [9] or constant switching frequency controllers [8], [10].

In addition to power control of DFIG, some researchers study synchronization of DFIGs [11-13] to minimize the difference between the grid voltages and the stator voltages before the generators are connected to the grids. Similar to power control, FOC can be used to synchronize DFIGs with cascaded inner current control loops and outer voltage control loops. Moreover, DTC for synchronization is proposed in [12], in which the stator is controlled by inner flux control loops and outer frequency and voltage control loops.

It is also worth noting that even there are prior arts on power control and synchronization of DFIGs, the control of the transition from synchronization to power generation of DFIGs is hardly mentioned.

In this paper, the topology of a typical DFIG system is presented. The mathematical model and equivalent circuit of the DFIGs in various operating stages are provided to describe the operation of DFIGs. Investigations on the effect of different state transition delays are then performed. Finally, a strategy to optimize the transition is proposed with experimental verification.

II. Topology

Fig 1 shows the topology of a typical DFIG system. The grid-side converter is a bi-directional inverter, which regulates the DC-link voltage by controlling the power flow between the DC-link and the power grid. The DC-link controller monitors the DC-link voltage, the grid voltage v_g and the current flow between the converter and the grid to control the switching of the converter. The rotor-side converter controls the voltage acting on the rotor winding of the DFIG. The machine controller monitors the rotor current i_r, stator current i_s, stator voltage v_s, and rotor angle θ_r to control the switching of the rotor-side converter. To control objective of the machine controller during synchronization, when the contactor is open, is to equalize the stator voltage and the grid voltage irrespective of the rotor speed. During power generation, when the contactor is closed, the primary objective of the machine controller is to regulate the torque and reactive power of the DFIG.
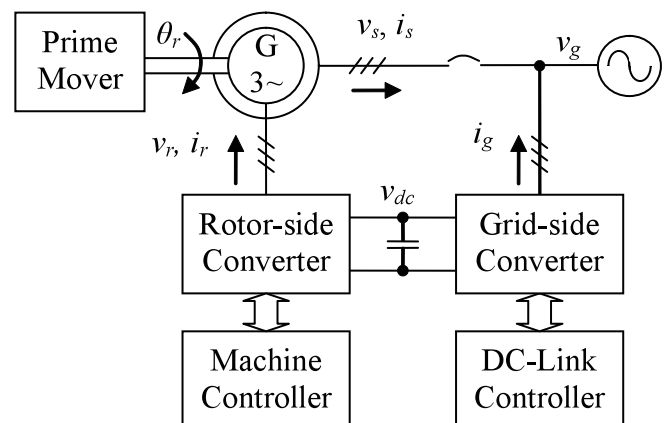

Fig 1: Topology of a DFIG system

III. MATHEMATICAL MODEL

In the grid voltage reference frame, the following equations describe the operation of a DFIG:

$$\overline{v}_{gxy} = \left| \overline{v}_{gxy} \right| \tag{1}$$

$$\overline{v}_{sxy} = \frac{d\overline{\lambda}_{sxy}}{dt} + j\omega_s \overline{\lambda}_{sxy} \tag{2}$$

$$\overline{v}_{rxy} = \overline{i}_{rxy} R_r + \frac{d\overline{\lambda}_{rxy}}{dt} + j(\omega_s - p\omega_r)\overline{\lambda}_{rxy} \tag{3}$$

$$\overline{\lambda}_{rxy} = (L_m + L_{r\sigma})\overline{i}_{rxy} \tag{4}$$

$$\overline{\lambda}_{sxy} = L_m \overline{i}_{rxy} \tag{5}$$

$$\omega_r = \frac{d\theta_r}{dt} \tag{6}$$

whereas λ_s is the stator flux linkage, λ_r is the rotor flux linkage, t is the time, R_r is the rotor resistance, L_m is the magnetizing inductance, $L_{r\sigma}$ is the rotor leakage inductance, ω_s is the grid frequency, ω_r is the rotor speed. Subscript xy shows that the variables are in the grid voltage reference frame. The corresponding equivalent circuit is shown in Fig 2, in which the stator leakage inductance and winding resistance are represented by $L_{s\sigma}$ and R_s respectively.
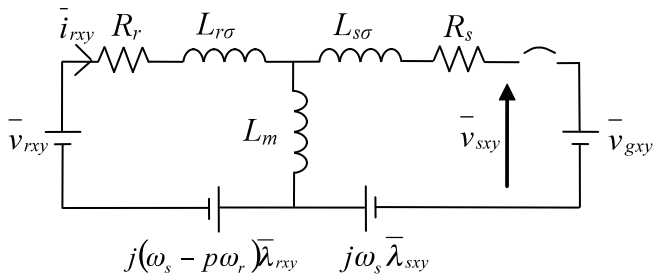

Fig 2: Equivalent circuit during synchronization

The operation of the DFIG during power generation is described by the following equations and (6):

$$\overline{v}_{s\alpha\beta} = \left| \overline{v}_{s\alpha\beta} \right| = R_s \overline{i}_{s\alpha\beta} + \frac{d\overline{\lambda}_{s\alpha\beta}}{dt} + j\omega_s \overline{\lambda}_{s\alpha\beta} \tag{7}$$

$$\overline{v}_{r\alpha\beta} = R_r \overline{i}_{r\alpha\beta} + \frac{d\overline{\lambda}_{r\alpha\beta}}{dt} + j(\omega_s - p\omega_r)\overline{\lambda}_{r\alpha\beta} \tag{8}$$

$$\overline{\lambda}_{s\alpha\beta} = (L_{s\sigma} + L_m)\overline{i}_{s\alpha\beta} + L_m \overline{i}_{r\alpha\beta} \tag{9}$$

$$\overline{\lambda}_{r\alpha\beta} = L_m \overline{i}_{s\alpha\beta} + (L_{r\sigma} + L_m)\overline{i}_{r\alpha\beta} \tag{10}$$

Subscript $\alpha\beta$ indicates variables in the stator flux frame. The corresponding equivalent circuit is shown in Fig 3.

IV. SIMULATION STUDIES

To investigate the effects of the delay in the state transition of the DFIG from synchronization to power generation, the synchronization algorithm and current control algorithm for power generation are implemented in [11] with a rotor position sensor and with different delay

times. As the closing delay time of a typical contactor is within the range of 15 ms to 40 ms, state transition time delays of 0 ms, 27.5 ms and 40 ms are studied in order to find the optimal transition time. The simulation platform is Matlab/Simulink and the simulated contactor delay time is 27.5 ms.
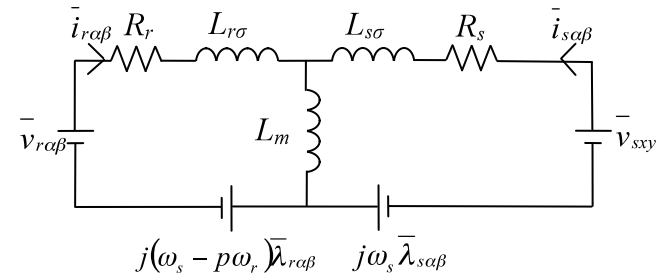

Fig 3: Equivalent circuit during power generation

1. No Delay Time

The stator and rotor current waveforms at the instant of state transition are shown in Fig 4. The DFIG is operating at 1400 RPM, and the grid and stator voltages are 200 V. The state transition occurs at 0.2 s and the magnitudes of both stator and rotor currents increase rapidly. The maximum magnitude of the rotor current is 11.38 A, while that of the stator current is 4.59 A. It can be seen that the magnitudes of the rotor and stator currents converge to their steady state values of 1.1 A and 1.02 A, respectively.
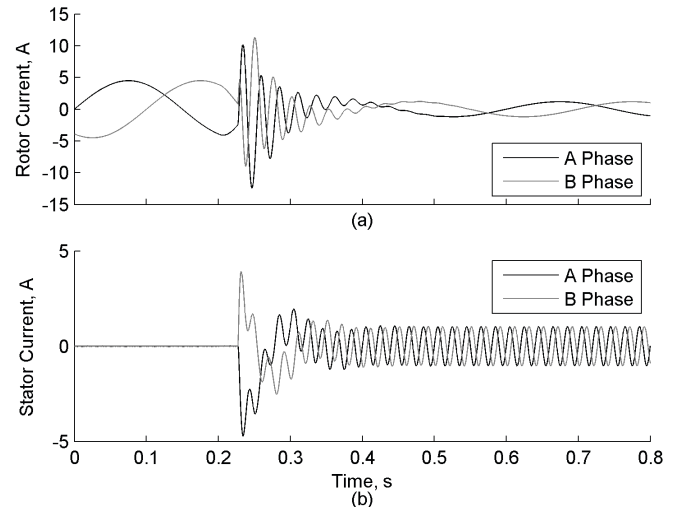

Fig 4: Current waveforms with no delay in state transition

2. Mean Delay Time

Simulation is performed with a matched state transition delay of 27.5 ms as shown in Fig 5. When the transition occurs at 0.2 s, the contactor is closed at the same time. There is no overshoot in both rotor and stator currents throughout the simulation.

3. Maximum Delay Time

Simulation results with a delay time of 4 ms are shown in Fig 6. It is observed that there is no overshoot in both currents also. Therefore, one may conclude that the there will be no current stresses if the state transition occurs after than the closing of the contactor, and it would be preferable to have long delays for the state transition as

the closing time of the contactor may change. However, if there are deviations between the measured stator voltage and grid voltage during synchronization, which are common as the two voltages are acquired with different sensors, the synchronization controller will act on the deviations and generate excessive currents when the contactor is closed. The phenomenon is observed in the simulation results shown in Fig 7 which assumes that there is a 5% error in the acquired stator voltage and the contactor is not closed. Therefore, excessive delay time should not be used.
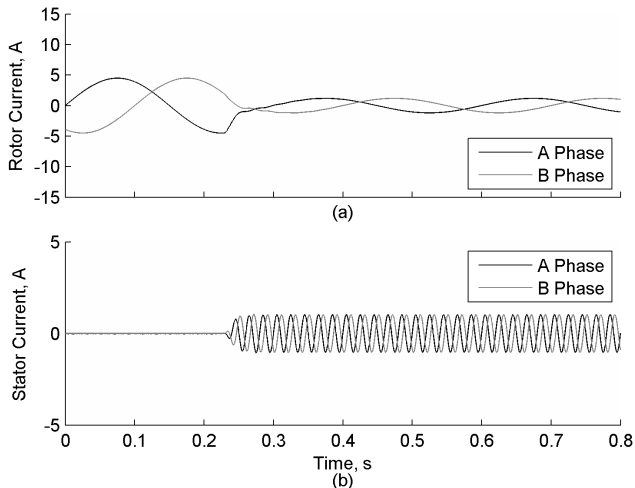

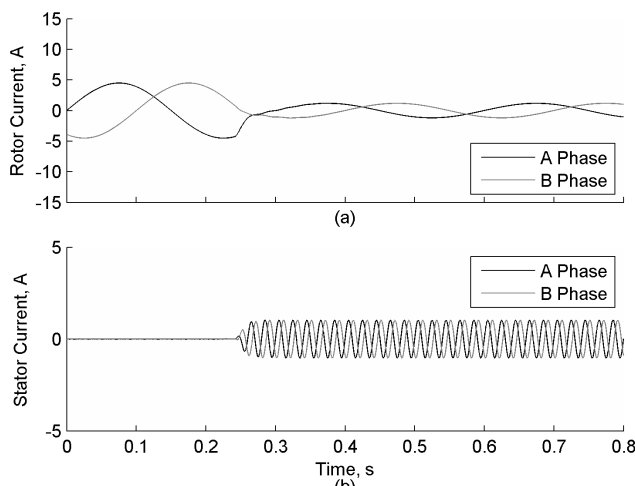Fig 5: Current waveforms with 27.5 ms delay in state transition

Fig 6: Current waveforms with 4 ms delay in state transition

4. Optimal Delay Time

A scheme with a feedback of the status of the contactor is proposed to control the transition of the operating state from synchronization to power generation. The transition is performed only if the contactor is confirmed to have closed. As shown in Fig 8, there is no current overshoot in the transition. Similar results are obtained for different delay times of the contactor. It offers the additional advantage of protecting the generator by ensuring the DFIG would not operate in the power generation state if the contactor fails to close due to whatever reasons.

V. EXPERIMENTAL RESULTS

The proposed scheme with the feedback of the contactor state is implemented with a prototyping card dSpace DS1104. The sampling frequency is 2 kHz. The DFIG operates at 1400 RPM with the stator and grid voltages being 200 V. Fig 9 shows the experimental waveforms. The maximum magnitude of the rotor current is 6.04 A, and there is no observable overshoot in the stator current. Similar waveforms with no current overshoot are observed when the DFIG is operating at the rated stator voltage of 380 V as shown in Fig 10.

VI. CONCLUSION

In this paper, the current stress in relation to the time difference between the closing of the stator side contactor and the transition of the operating state of the DFIG controller are investigated. From the simulation, it is observed that there are overshoots in the stator and rotor currents if the state transition occurs before the closing of the contactor. If the state transition occurs on or after the closing of the contactor, there is no overshoot. However, excessive delay in the state transition may introduce undesirable large currents. A state transition with the feedback of the contactor state is thus proposed to match the state transition time with the contactor closing time.
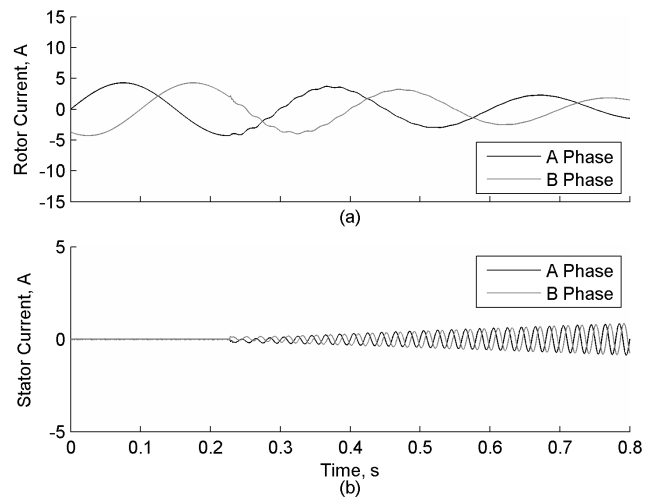

Fig 7: Current waveforms with no state transition and 5% error in the acquired stator voltage
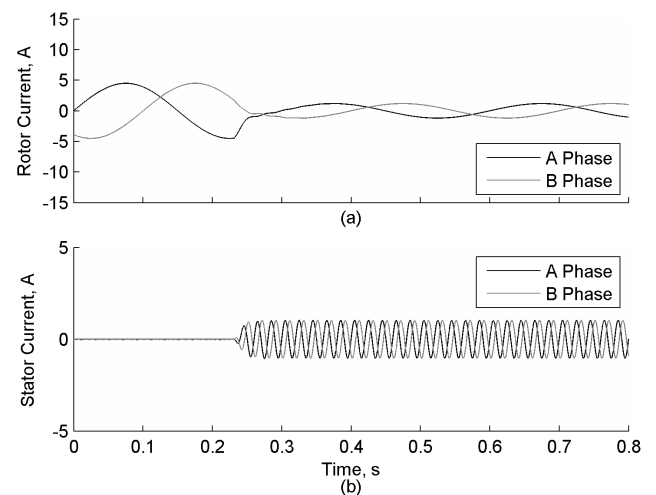

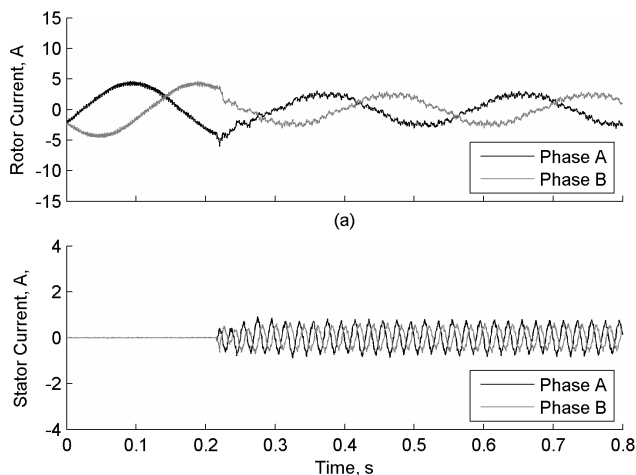Fig 8: Current waveforms with feedback of the contactor state.

Fig 9: Current waveforms with feedback of the contactor state at the stator voltage of 200 V.
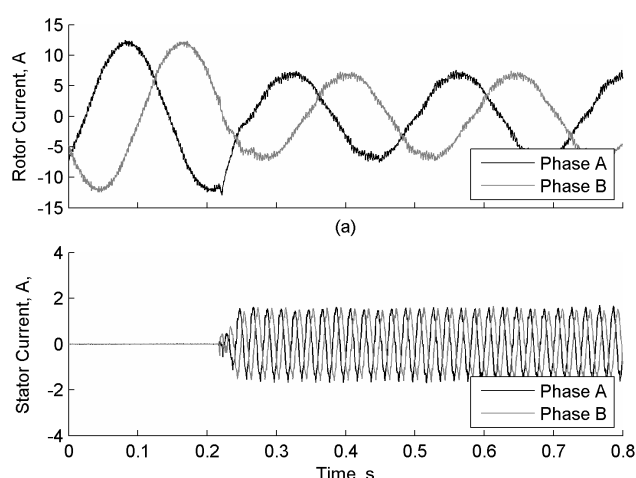

Fig 10: Current waveforms with feedback of the contactor state at the stator voltage of 380 V.

APPENDIX

Machine Parameters
Stator rated voltage: 380 V
Stator rated current: 4.5 A
Rotor rated voltage: 120 V
Rotor rated current: 10 A
Operating frequency: 50 Hz
Synchronous speed: 1500 rpm
Magnetizing inductance (referred to the stator): 0.3498 H
Rotor leakage inductance (referred to the stator): 0.0219 H
Stator leakage inductance: 0.0219 H
Rotor winding resistance (referred to the stator): 5.317 Ω
Stator winding resistance per phase: 2.670 Ω
Stator to rotor turn ratio: 3.03

REFERENCES

[1] Mutschler, P., and Hoffmann, R.: 'Comparison of wind turbines regarding their energy generation'. IEEE 33rd Annual Power Electronics Specialists Conference, Queensland, Australia, June 2002, pp. 6-11.

[2] Hulle, F.V.: 'Large scale integration of wind energy in the European supply: analysis, issues and recommendations' (European Wind Energy Association, 2005)

[3] Tamura, J., Sasaki, T., Ishikawa, S., and Hasegawa, J.: 'Analysis of the steady state characteristics of doubly fed synchronous machines', IEEE Trans. Energy Convers., Vol. 4, No. 2, 1989,pp. 250-256

[4] Boldea, I.: 'Variable speed generators: the electric generators handbook' (Taylor & Francis, 2006), Ch. 2

[5] Tang, Y., and Xu, L.: 'A flexible active and reactive power control strategy for a variable speed constant frequency generating system', IEEE Trans. Power Electron., Vol. 10, No. 4, 1995, pp. 472-478

[6] Tapia, A., Tapia, G., Ostolaza, J.X., and Sáenz, J.R.: 'Modeling and control of a wind turbine driven doubly fed induction generator', IEEE Trans. Energy Convers., Vol. 18, No. 2, 2003, pp. 194-204

[7] Arnalte, S., Burgos, J.C., and Rodríguez-Amenedo, J.L: 'Direct torque control of a doubly-fed induction generator for variable speed wind turbines', Electric Power Components and Systems, Vol. 30, No. 2, 2002, pp. 199-216

[8] Wong, K.C., Ho, S.L., and Cheng, K.W.E.: 'Direct torque control of a doubly-fed induction generator with space vector modulation', Electric Power Components and Systems, Vol. 36, No. 12, 2008, pp. 1337-1350

[9] Arnalte, S., and Rodríguez-Amenedo, J.L: 'Sensorless direct power control of a doubly fed induction generator for variable speed wind turbines'. European Power Electronics and Drives Association 10th International Conference on Power Electronics and Motion Control, Cavtat and Dubrovnik, Croatia, September 2002, pp. 1-12

[10] Zhi, D., and Xu, L.: 'Direct power control of DFIG with constant switching frequency and improved transient performance', IEEE Trans. Energy Convers., Vol. 22, No. 1, 2007, pp. 110-118

[11] Morel, L., Godfroid, H., Mirzaian, A., and Kauffmann, J.M.: 'Double-fed induction machine: converter optimisation and field oriented control without position sensor', IEE Proc. Electr. Power Appl., Vol. 145, No. 4, 1998, pp. 360-368

[12] Gómez, S.A, and Amenedo, J.L.R.: 'Grid synchronisation of doubly fed induction generators using direct torque control'. IEEE 28th Annual Conference of the Industrial Electronics Society, Sevilla, Spain, November 2002, pp. 3338-3343

[13] Wong, K.C., Ho, S.L., and Cheng, K.W.E.: 'Direct voltage control for grid synchronization of doubly fed induction generators', Electric Power Components and Systems, Vol. 36, No. 9, 2008, pp. 960-976